

Article

Effect of Mn Content on the Reaction between Fe-xMn (x = 5, 10, 15, and 20 Mass pct) Steel and CaO-SiO₂-Al₂O₃-MgO Slag

Huixiang Yu ^{1,*}, Muming Li ², Jiaming Zhang ¹ and Dexin Yang ¹

¹ School of Metallurgical and Ecological Engineering, University of Science and Technology Beijing, 30 Xueyuan Road, Haidian District, Beijing 100083, China; zhangjiaming0086@163.com (J.Z.); Y717977560@163.com (D.Y.)

² Chongqing Iron and Steel Designing Institute Information Co., Ltd., Chongqing 401122, China; Muming.Li@cisdi.com.cn

* Correspondence: yuhuixiang@ustb.edu.cn

Abstract: Medium- and high-Mn steels have excellent properties but are very difficult to be commercially produced because of the high content of some alloy elements. To enhance the understanding of the reaction between medium/high-Mn steel and refining slag which is significantly different from the conventional steels, steel and slag composition and the inclusions were investigated by equilibrium reaction between Fe-xMn (x = 5, 10, 15, and 20 mass pct) and CaO-SiO₂-Al₂O₃-MgO top slag at 1873 K in the laboratory. Furthermore, the effect of Mn content on inclusion transformation and steel cleanliness was also explored. After slag-steel reaction, both contents of MnO in slag and Si in steel increased. Most MnO inclusions in master steel transformed to MnO-SiO₂ and MnO-Al₂O₃-MgO. With the increase in Mn content, the amount share of MnO type inclusions decreased and that of MnO-Al₂O₃-MgO type increased. In addition, both the number density of observed inclusions and the calculated oxygen content in inclusions increased. Thermodynamic analysis indicates that the composition change of steel and slag and the transformation of inclusions are mainly the consequence of the reaction between Mn in molten steel and SiO₂ and MgO in top slag. The dissolved Mn in medium/high-Mn steel presents a strong reactivity.

Keywords: medium/high-Mn steel; Mn content; nonmetallic inclusion; interaction mechanism; slag-steel reaction



Citation: Yu, H.; Li, M.; Zhang, J.; Yang, D. Effect of Mn Content on the Reaction between Fe-xMn (x = 5, 10, 15, and 20 Mass pct) Steel and CaO-SiO₂-Al₂O₃-MgO Slag. *Metals* **2021**, *11*, 1200. <https://doi.org/10.3390/met11081200>

Academic Editor: Marcello Cabibbo

Received: 16 June 2021

Accepted: 17 July 2021

Published: 28 July 2021

Publisher's Note: MDPI stays neutral with regard to jurisdictional claims in published maps and institutional affiliations.



Copyright: © 2021 by the authors. Licensee MDPI, Basel, Switzerland. This article is an open access article distributed under the terms and conditions of the Creative Commons Attribution (CC BY) license (<https://creativecommons.org/licenses/by/4.0/>).

1. Introduction

In the past decades, with the increasing desire for energy saving and environmental protection, medium- and high-Mn steels, with Mn content higher than 3%, have garnered great attention from the automotive industry and researchers due to their outstanding mechanical properties, broad application prospects, and very high production difficulties.

Some studies in metallurgy have been conducted to explore the mechanism, fundamental data, etc. for medium/high-Mn steels and to solve the problems met during the production of these steels. Pak [1] studied the thermodynamics of deoxidation equilibria and AlN formation in high-Mn- and high-Al-alloyed liquid steel. Yan [2] and Yu [3] investigated metallurgical characteristics of refining slag for high-manganese steel. Kim et al. [4,5] studied reactions between Al and Mn in liquid steel and molten mold flux, which is closely related to the difficulties met in continuous casting of medium/high-Mn steels. With regard to the studies in the field of steelmaking, Liu [6] investigated the effect of CO₂ and O₂ mixed injection on Mn retention in high-Mn steel. Gigacher [7] and Alba [8] investigated the inclusions in high-Mn steel with different Mn content or Al content in absence of top slag. As known, ladle slag is used in the production of medium/high-Mn steels. Because of the high content of alloys in these steels, the reactions between molten steel and top

slag are significantly different from those of conventional steels. Yu [3] investigated the refining slag CaO-SiO₂-Al₂O₃-MgO in equilibrium with Fe-(10, 20 mass pct)Mn. The MnO content in slag is much higher than that in equilibrium with conventional steel because of the reaction between [Mn] in steel and SiO₂ in slag. Peymandar [9] studied the reaction between CaO-SiO₂-Al₂O₃-MgO slag (initial slag basicity = 1.3, Al₂O₃ = 15 mass pct) and high-Mn steel, with a focus on reaction kinetics. Deng [10] studied the reaction between Al-killed manganese steel and CaO-SiO₂-Al₂O₃-MgO ladle slag. Strong reactions between [Al] and [Mn] in steel and SiO₂ and MgO in slag were observed in both above studies. Such reactions are also reported in Yu's studies [11,12]. So, Mn in medium/high-Mn steels has strong reactivity and plays an important role in the reaction between steel and top slag. It is well known that the reaction between molten steel and top slag has a great effect on the precise control of steel composition and improvement of cleanliness [13–16]. However, the effects of Mn content on the reaction between medium/high-Mn steels and ladle slag have received little attention and seldom been reported. In addition, inclusions were seldom investigated in the above studies.

In the present work, the reaction between medium/high-Mn Steel, with Mn content of 5, 10, 15, and 20 mass pct, and CaO-SiO₂-Al₂O₃-MgO slag was investigated at 1873 K by laboratory equilibrium experiments. The composition evolution of steel and slag and the nonmetallic inclusions were analyzed. Based on the experimental results, the effects of Mn content on inclusion transformation and steel cleanliness are discussed with the aid of thermodynamic calculations.

2. Experimental

2.1. Materials

Four master steels, with nominal Mn content of 5, 10, 15, and 20 mass pct were employed for slag–steel reaction experiments, which were prepared by using electrolytic iron and electrolytic manganese. Table 1 gives the composition of raw metal materials, in which the composition of electrolytic iron is from certificate and that of electrolytic manganese is by measurement with the following methods: Si by ICP-AES, Al by ICP-MS, and S by infrared absorption method. Initial slag was CaO-SiO₂-Al₂O₃-MgO system with 20% Al₂O₃, 6% MgO, and slag basicity ($B = \text{CaO}/\text{SiO}_2$) of 4 by mixing chemical analytical reagents.

Table 1. Compositions of raw metal materials, mass%.

Material	Impurity Elements					
	C	Si	Al	S	O	N
Electrolytic iron	0.0005	<0.0005	<0.001	0.0006	0.008	<0.0005
Electrolytic manganese	-	0.026	0.018	0.01	-	-

2.2. Experimental Method

Experiments were carried out in a vertical electric resistance furnace with Si-Mo heating, the schematic of which is shown in Figure 1. First, 180 g master steel and 36 g initial slag were charged together into a MgO crucible, which was then put in the constant temperature zone of an alumina reaction chamber. Heating began, and the moment when 1873 K was reached was set as the starting time of reaction. After slag and steel reacted for 90 min, which was determined by the preliminary experiment, the MgO crucible was taken out and water-cooled quickly. The whole experiment was carried out under argon protective atmosphere. The detailed experimental procedure is described in the authors' previous studies [3,12]. According to different Mn contents, the experiments were divided into four groups, named Fe-5Mn, Fe-10Mn, Fe-15Mn, and Fe-20Mn.

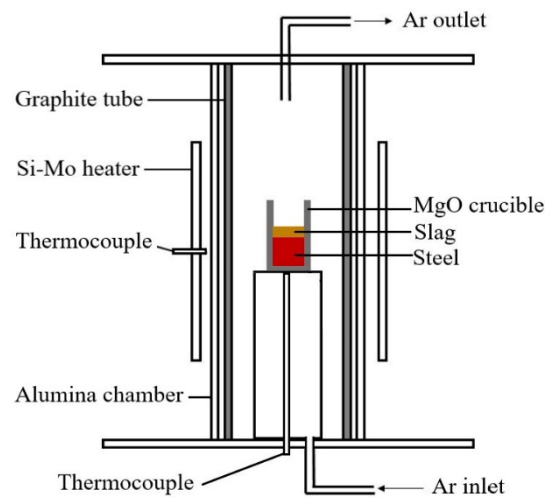


Figure 1. Schematic of experimental set-up.

Chemical compositions of the obtained steel and slag samples were analyzed and nonmetallic inclusions were detected by a scanning electron microscope (SEM, JEOL JSM-6480LV) equipped with EDS (Thermo-NS6) and Aspek PSEM Explorer (ASPEX for short; Aspek Corporation). Total oxygen content (T.O) of steel was analyzed by hydrogen/nitrogen/oxygen determinator (TCH600, LECO Corporation, Saint Joseph, MI, USA). For the ASPEX observation of inclusions in the present work, the detected minimum inclusion size was set as 1 μm , and an area of no less than 20 mm^2 for each steel sample was observed to obtain statistical information. The program parameters of ASPEX for inclusion detection, beam energy, emission current, and working distance were set at 20 kV, 43.5 μA , and 17 mm, respectively. The detailed analysis methods are described in the authors' previous studies [12,17].

3. Experimental Results

3.1. Chemical Compositions of Slag

Chemical compositions of slag samples after slag–steel reaction are shown in Table 2. A notable change in slag composition is that MnO content increased greatly from zero to 4.06–5.44% in the present study. The initial and final slag compositions with different Mn contents were plotted in the phase diagram of the multicomponent system (the CaO-SiO₂-Al₂O₃-6%MgO-5%MnO system), which was calculated by FactSage 7.1, as shown in Figure 2. The compositions of the final slags of the four groups were located near the saturated line of (Mn, Mg)O, and the final slag of Exp. Fe-5Mn was a little different from those of Exp. Fe-10Mn, Fe-15Mn, and Fe-20Mn [12].

Table 2. Chemical composition of slag samples after equilibrium, mass%.

Exp. No.	CaO	SiO ₂	Al ₂ O ₃	MgO	MnO	FeO
Fe-5Mn	51.53	15.76	20.01	7.77	4.25	0.84
Fe-10Mn	53.66	15.02	18.88	7.81	4.06	0.56
Fe-15Mn	53.48	14.22	19.39	7.68	4.77	0.53
Fe-20Mn	53.49	14.48	18.91	7.39	5.44	0.45

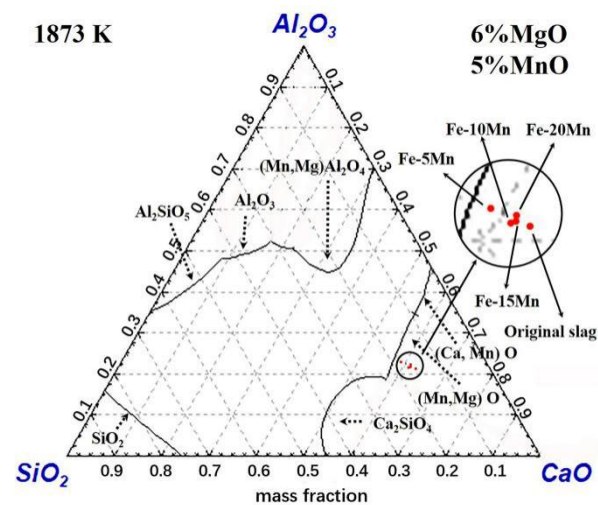


Figure 2. Change in slag compositions before and after slag–steel reaction.

3.2. Chemical Compositions of Steel

Chemical compositions of steel samples after slag–steel reaction are shown in Table 3. The analyzed Mn contents were a little lower than the preset values. It also indicated that Mn yield improved with the increase in Mn content. Electrolytic manganese, which was used in this study, contains a few impurity elements, Al, Si, and S. Consequently, small amounts of these elements were taken into the steel bath with electrolytic manganese. Table 4 gives the calculated chemical composition of initial steel samples. After slag–steel reaction, Si content increased and S decreased. Furthermore, the increase in Si was higher than the amount that was taken in by electrolytic manganese and increased with the increase in Mn content in steel.

Table 3. Chemical composition of steel samples after equilibrium, mass%.

Exp. No.	Mn	Al	Si	S	T.O	Mn Yield, %
Fe-5Mn	4.23	0.0026	<0.005	0.0007	0.0022	84.60
Fe-10Mn	9.20	0.0025	0.0091	0.0004	0.0018	92.00
Fe-15Mn	14.51	0.0024	0.015	0.0004	0.0022	96.73
Fe-20Mn	19.76	0.0028	0.02	0.0007	0.0023	98.80

Table 4. Calculated initial chemical composition of steel, mass%.

Exp. No.	Mn	Al	Si	S	O	Fe
Fe-5Mn	5	0.0019	0.0018	0.0011	0.0077	Bal.
Fe-10Mn	10	0.0028	0.0031	0.0016	0.0072	Bal.
Fe-15Mn	15	0.0036	0.0044	0.0021	0.0068	Bal.
Fe-20Mn	20	0.0045	0.0058	0.0025	0.0064	Bal.

The reason for the increase in Si content in steel and MnO in slag is discussed in the authors' previous studies [3,12]. During the reaction between top slag and molten steel, Equation (1) occurred [16,18].



$$\Delta G_1 = 5700 + 34.8 T \text{ J/mol} \quad (2)$$

$$K_1 = \frac{a_{(\text{MnO})}^2 \cdot a_{[\text{Si}]}}{a_{[\text{Mn}]}^2 \cdot a_{(\text{SiO}_2)}} \quad (3)$$

$$\log K_1 = 2 \log a_{(\text{MnO})} - \log a_{(\text{SiO}_2)} + \log a_{[\text{Si}]} - 2 \log a_{[\text{Mn}]} \quad (4)$$

$$a_i = f_i \cdot \%i \quad (5)$$

where $a_{[i]}$ or $a_{(i)}$ is the activity of i in molten steel or slag and K_1 is the equilibrium constant of Equation (1).

Assuming the slag–steel reaction has reached equilibrium, the ratio of MnO to SiO₂ of slags, $\log(a_{(\text{MnO})}^2/a_{(\text{SiO}_2)})$, is expected to exhibit a linear relation to the $\log(a_{[\text{Mn}]}^2/a_{[\text{Si}]})$ of steel melts with the slope of unity at a fixed temperature. The $a_{(\text{MnO})}$, $a_{(\text{SiO}_2)}$, $a_{[\text{Mn}]}$, and $a_{[\text{Si}]}$ of the four sets of experiments with different Mn contents were calculated. Here, $a_{(\text{MnO})}$ and $a_{(\text{SiO}_2)}$ were calculated by FactSage 7.1, and $a_{[\text{Mn}]}$ and $a_{[\text{Si}]}$ were calculated by Equation (5) (Tables 3 and 5). Figure 3 shows the $\log(a_{(\text{MnO})}^2/a_{(\text{SiO}_2)})$ of final slags as a function of $\log(a_{[\text{Mn}]}^2/a_{[\text{Si}]})$ of steel melts after slag–steel reaction. The $\log(a_{(\text{MnO})}^2/a_{(\text{SiO}_2)})$ of slags linearly increases by increasing the $\log(a_{[\text{Mn}]}^2/a_{[\text{Si}]})$ of steel melts with the slope of 0.75. Thus, it can be inferred that the slag–steel system investigated in this work was in thermodynamic equilibrium [19].

Table 5. Interaction coefficients used in thermodynamic calculation [16,20,21].

e_i^j	Al	Si	Mn	O	S	C
Si	0.058	0.11	0.002	−0.23	0.056	0.18
Mn	−0.012	0	0	−0.083	−0.048	−0.07
O	-	−0.131	−0.021	−1750/T + 0.76	−0.133	-

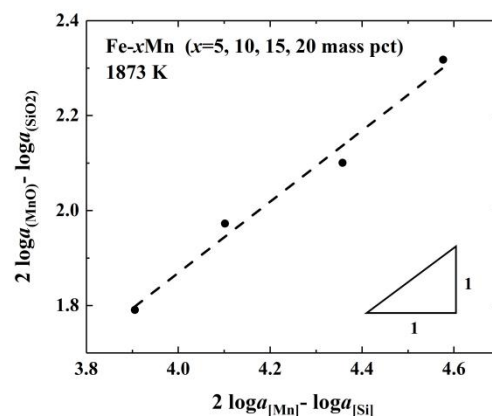


Figure 3. Composition of slags, $\log(a_{(\text{MnO})}^2/a_{(\text{SiO}_2)})$ as a function of $\log(a_{[\text{Mn}]}^2/a_{[\text{Si}]})$ in Fe-xMn melts at 1873 K.

3.3. Analysis of Inclusions

3.3.1. Inclusion Type

The inclusions in steel samples were analyzed by ASPEX. The observed area of samples Fe-5Mn, Fe-10Mn, Fe-15Mn, and Fe-20Mn were 27.56, 25.59, 32.15, and 23.46 mm², and the numbers of detected inclusions were 669, 752, 1406, and 1268, respectively. Inclusions in master medium- and high-Mn steels are mainly MnO type. Some contain a little Al₂O₃ and MnS [3]. After the reaction with the top slag of the CaO-SiO₂-Al₂O₃-MgO system, most inclusions transformed into three types, which were MnO-SiO₂, MnO-Al₂O₃-MgO, and MnO types, with the MnO-SiO₂ type representing the majority; the typical morphologies of the three types of inclusions are shown in Figure 4. With the increase of Mn content, there was little change in inclusion types. That is, the above three types of inclusions existed in steel samples of the four groups of experiments after slag–steel reaction.

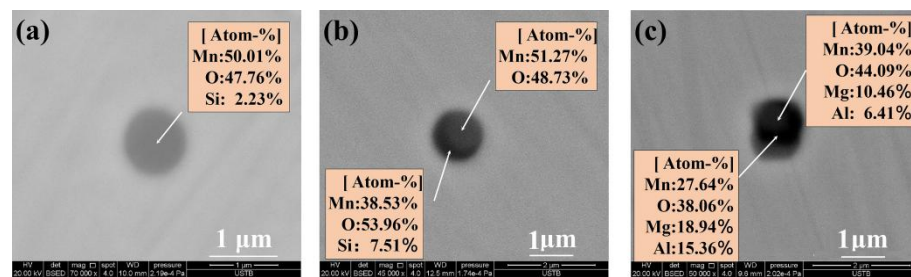


Figure 4. Morphology of typical inclusions after slag–steel reaction: (a) MnO; (b) MnO-SiO₂ system; (c) MnO-Al₂O₃-MgO system.

3.3.2. Effect of Mn Content on Inclusion Type

The statistical information of inclusions in steel samples was obtained by ASPEX. Inclusion types change little with Mn content increasing, whereas, the amount proportion of each type changed greatly, as shown in Figure 5. The percentage of MnO type decreased and MnO-Al₂O₃-MgO type increased with the increase in Mn content. The contents of Mg, Al, Si, Ca, Mn, and S of the detected inclusions were recounted to the sum of 100%. Figure 6 shows the average mass percentages of main elements in inclusions. It is easily seen that Mn represents the majority in inclusions. With the increase in Mn content, Mn content in inclusions shows a decreasing trend while Al and Mg show an increasing trend.

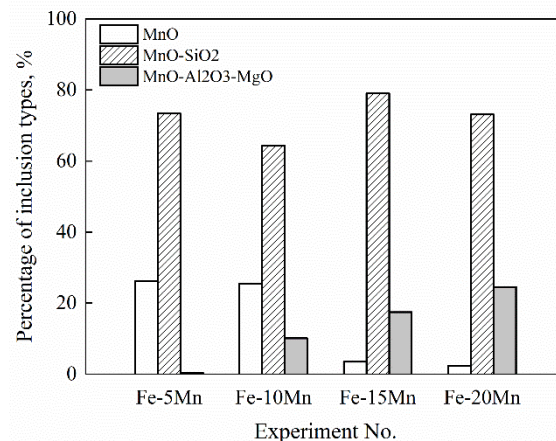


Figure 5. Percentage of inclusion types.

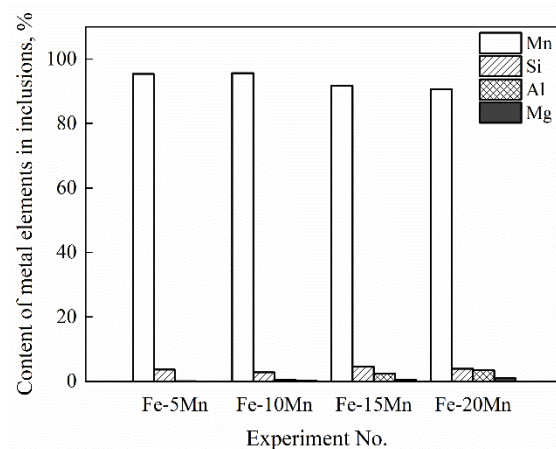


Figure 6. Average contents of main elements in the detected inclusions.

3.3.3. Relationship between Mn Content and Steel Cleanliness

With the increase in Mn content from 5% to 10%, 15%, and 20%, total oxygen content (T.O) changed from 22.4×10^{-6} to 17.6×10^{-6} , 21.5×10^{-6} , and 23.2×10^{-6} , which shows

no apparent tendency. The number density of inclusions in steel increased with the increase in Mn content, as shown in Figure 7.

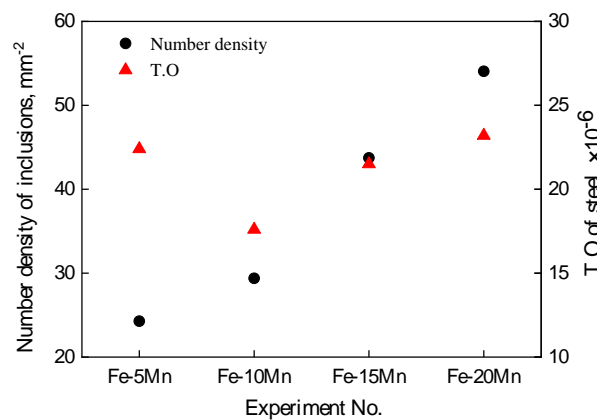


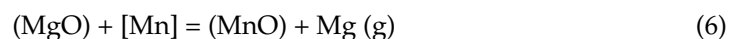
Figure 7. T.O content of steel and number density of inclusions.

4. Discussion

4.1. Evolution Mechanism of Inclusions

After reaction with CaO-SiO₂-Al₂O₃-MgO top slag, the main type of inclusions transformed from MnO in master steel to MnO-SiO₂. This is because the reaction $[Mn] + (SiO_2) = [Si] + (MnO)$ occurred between medium/high-Mn steel and top slag, which is explored in detail in the authors' previous studies [3]. In the present study, the change in Gibbs free energy of Reaction (1) with different Mn content was calculated, and the values were -73759.5 , -88791.4 , -99322.9 , and -106335.8 J/mol for Exp. Fe-5Mn, Fe-10Mn, Fe-15Mn, and Fe-20Mn, respectively. In the thermodynamic calculations, activities of slag components were obtained by FactSage 7.1. The values calculated for the four groups of experiments are all negative, which indicates that Reaction (1) could occur. That is, in this study, the high content of Mn in molten steel would react with SiO₂ in slag to supply [Si] to the steel bath, which makes MnO inclusion transform to MnO-SiO₂.

Another phenomenon is that, with the increase in Mn content in steel, the proportion of MnO type decreased greatly and that of MnO-Al₂O₃-MgO type increased, as shown in Figure 5. As reported in Deng's research [10], when the Mn content is high enough, for example, $w(Mn) = 20\%$, the dissolved Mn can not only reduce SiO₂ in slag but also react with MgO in slag. Park [22] investigated the reaction between CaO-SiO₂-MgO-Al₂O₃ flux and Fe-xMn-yAl ($x = 10$ and 20 mass pct, $y = 1, 3$, and 6 mass pct) steel at 1873 K. Several small solid compounds, i.e., [Mg, Mn]Al₂O₄ spinel, were found in the slag reacted with Fe-20Mn-1Al but not found in the slag with Fe-10Mn-1Al. Therefore, the dissolved Mn in molten steel presents strong reactivity with the increase in Mn content. In the present study, Reaction (6) would occur with the increase in Mn content [10,23]. MgO in slag would be reduced by Mn in steel, and then the generated Mg would combine with oxygen in the steel bath or existing inclusions. As a result, inclusions of MnO-Al₂O₃-MgO type formed.



$$\Delta G_2 = 325,340 - 80.2 T \text{ J/mol} \quad (7)$$

4.2. Effect of Mn Content on Steel Cleanliness

Alba [8] investigated the inclusions in Fe-xMn-3%Al ($x = 2\%$, 5% , 20%) steel in absence of top slag. In his research, the observed inclusions were mainly Al₂O₃ (pure), Al₂O₃-MnS, AlN (pure), AlN-MnS, AlON-MnS, AlON, and MnS. With the increase in Mn content, the total amount of inclusions increased, and the increase was mainly in the number of AlN and MnS inclusions. In the present study, T.O showed no apparent tendency, while the number density of inclusions increased with the increase in Mn content in steel, as shown

in Figure 7. To clarify the effect of Mn content on steel cleanliness, dissolved oxygen in steel and oxygen in inclusions were calculated, and then the relationship between T.O, oxygen in inclusions, and number density of inclusions was explored with the increase in Mn content.

T.O in steel is the sum of the free oxygen content ($[O]_{\text{free}}$) and the oxygen content in the inclusions ($(O)_{\text{inc}}$), as shown in Equation (8). In this study, the Mn content of steel was high, and the main component of the inclusions was MnO, so it can be assumed that the free oxygen content in the steel bath was controlled by manganese–oxygen equilibrium, as shown in Reaction (9) [24].

$$\text{T.O} = [O]_{\text{free}} + (O)_{\text{inc}} \quad (8)$$

where T.O is the total oxygen content of steel, $[O]_{\text{free}}$ is the free oxygen content in steel, and $(O)_{\text{inc}}$ is the oxygen content in the inclusions.



$$\Delta G_3 = -244,300 + 107.6T \text{ J/mol} \quad (10)$$

$$K_3 = \frac{a_{(\text{MnO})}}{a_{[\text{Mn}]} \cdot a_{[\text{O}]}} \quad (11)$$

where K_3 is the equilibrium constant of Reaction (9); $a_{(\text{MnO})}$, $a_{[\text{Mn}]}$, and $a_{[\text{O}]}$ are the activities of MnO in slag, Mn in molten steel, and O in molten steel, respectively.

According to Equations (5), (10), and (11); the compositions in Tables 2 and 3; and the respective interaction coefficients in Table 5, the free oxygen content in the steel bath with different Mn contents can be obtained, which is shown as the sign “□” in Figure 8. In the calculation, the $a_{(\text{MnO})}$ was calculated by FactSage 7.1; its value is 0.0788, 0.0799, 0.0888, and 0.0999 for Exp. Fe-5Mn, Fe-10Mn, Fe-15Mn, and Fe-20Mn, respectively.

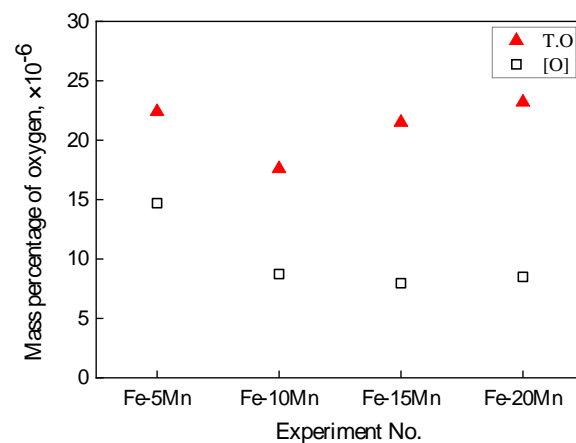


Figure 8. T.O and [O] content of steel.

As given in Equation (8), T.O of the steel is the sum of the free oxygen content and the oxygen content in the inclusions. Consequently, $(O)_{\text{inc}}$ can be obtained. Figure 9 shows the number density and oxygen content of the inclusions with different Mn contents. The change in the calculated oxygen content in the inclusions agrees well with that of the number density of the observed inclusions. With the increase in Mn content in steel, the oxygen content of inclusions and the number of observed inclusions per unit area increase, which indicates that the cleanliness of steel declines.

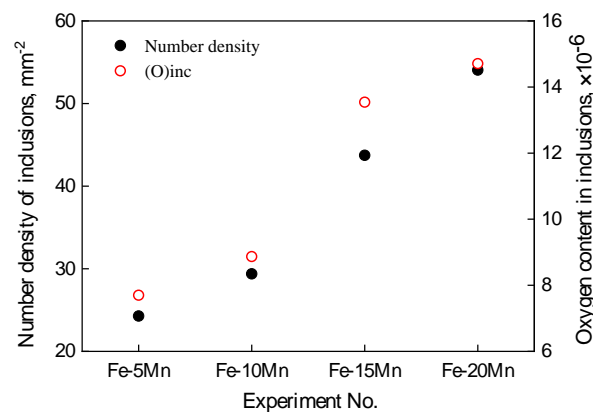


Figure 9. Number density and oxygen content of inclusions.

4.3. [O] in Equilibrium in Fe-xMn Melts

In the present study, the steel bath had a high content of Mn and a small amount of Si and Al solute elements, as given in Table 3. The detected inclusions in steel contained such components as MnO, SiO₂, and Al₂O₃. This indicates that the solute elements, Mn, Si, and Al, participate in the reactions in molten steel or between slag and steel. On the other hand, for the above calculation of oxygen content, the calculated dissolved oxygen content was less than the measured T.O content. Furthermore, the calculated oxygen content in inclusions agrees well with the number density of the observed inclusions under the assumption that Equation (9) is the main controlled reaction. So, all these results give strong evidence that the content of dissolved oxygen in this study is in equilibrium with Mn content in molten steel, although other metal elements, such as Si and Al, also participate in the reactions. That is, the dissolved oxygen content is controlled by Reaction (9).

After the reaction between top slag and molten steel, the main inclusions transformed from MnO to MnO-SiO₂ and MnO-Al₂O₃-MgO. Thermodynamic analysis shows that the reactions between Mn in molten steel and SiO₂ and MgO in top slag occur. The dissolved Mn in medium/high-Mn steel presents a strong reactivity.

5. Conclusions

Laboratory experiments were carried out to investigate the reaction between Fe-xMn ($x = 5, 10, 15,$ and 20 mass pct) and CaO-SiO₂-Al₂O₃-MgO refining slag. The following conclusions are drawn:

1. The dissolved Mn in medium/high-Mn steel presents a strong reactivity in the slag-steel reaction. The composition change of steel and slag and the transformation of inclusions are mainly the consequence of the reaction between Mn in molten steel and SiO₂ and MgO in top slag.
2. After slag-steel reaction, MnO content in slag increased greatly from zero to 4.06–5.44%, and Si content in steel increased. With the increase in Mn content in steel, the contents of MnO in slag and Si in steel show an increasing trend.
3. Most inclusions transformed from MnO in master steel to MnO-SiO₂ and MnO-Al₂O₃-MgO after reaction with top slag. With the increase in Mn content, the inclusion types show little change, while the amount share of MnO type inclusions decreased and that of MnO-Al₂O₃-MgO type increased.
4. With the increase in Mn content in steel, both the number density of the observed inclusions and the calculated oxygen content in inclusions increased, which indicates that the cleanliness of steel decreased.

Author Contributions: Conceptualization, H.Y., M.L.; methodology, H.Y., M.L.; software, J.Z., D.Y.; formal analysis, M.L., D.Y.; investigation, H.Y., M.L.; validation, H.Y., M.L.; writing—original draft preparation, H.Y., M.L.; writing—review and editing, H.Y., J.Z.; visualization, H.Y., M.L., J.Z., D.Y.; supervision, H.Y. All authors have read and agreed to the published version of the manuscript.

Funding: This research was funded by the Ministry of Industry and Information Technology of China (grant number TC180A6MR) and the National Key R&D Program of China (grant numbers 2017YFB0304000 and 2017YFB0304001).

Data Availability Statement: Not applicable.

Conflicts of Interest: The authors declare no conflict of interest. The sponsors had no role in the design, execution, interpretation, or writing of the study.

References

1. Paek, M.-K.; Do, K.-H.; Kang, Y.-B.; Jung, I.-H.; Pak, J.-J. Aluminum Deoxidation Equilibria in Liquid Iron: Part III—Experiments and Thermodynamic Modeling of the Fe-Mn-Al-O System. *Met. Mater. Trans. A* **2016**, *47*, 2837–2847. [[CrossRef](#)]
2. Yan, B.; Chen, X.; Tao, J. Activity of MnO in MnO-CaO-SiO₂-Al₂O₃-MgO Molten Slags. *Metall. Mater. Trans. B* **2017**, *48*, 1100–1107. [[CrossRef](#)]
3. Yu, H.; Yang, D.; Li, M.; Pan, M. Metallurgical characteristics of refining slag used for high manganese steel. *Met. Res. Technol.* **2019**, *116*, 620. [[CrossRef](#)]
4. Kim, M.S.; Park, M.S.; Kang, S.E.; Park, J.K.; Kang, Y.B. A Reaction between High Mn-High Al Steel and CaO-SiO₂-Type Molten Mold Flux: Reaction Mechanism Change by High Al Content ([pct Al]₀ = 5.2) in the Steel and Accumulation of Reaction Product at the Reaction Interface. *ISIJ Int.* **2018**, *58*, 686–695. [[CrossRef](#)]
5. Park, J.; Sridhar, S.; Fruehan, R.J. Kinetics of Reduction of SiO₂ in SiO₂-Al₂O₃-CaO Slags by Al in Fe-Al(-Si) Melts. *Met. Mater. Trans. A* **2014**, *45*, 1380–1388. [[CrossRef](#)]
6. Liu, H.; Liu, J.; Johannes, S.; Penz, F.M.; Sun, L.; Zhang, R.Z.; An, Z.G. Effect of CO₂ and O₂ Mixed Injection on the Decarburization and Manganese Retention in High-Mn Twinning-Induced Plasticity Steels. *Metall. Mater. Trans. B* **2020**, *51*, 756–762. [[CrossRef](#)]
7. Gigacher, G.; Krieger, W.; Scheller, P.R.; Thomser, C. Non-Metallic Inclusions in High-Manganese-Alloy Steels. *Steel Res. Int.* **2005**, *76*, 644–649. [[CrossRef](#)]
8. Alba, M.; Nabeel, M.; Dogan, N. Investigation of Inclusion Formation in Light-Weight Fe-Mn-Al Steels using Automated Scanning Electron Microscope Equipped with Energy-Dispersive X-Ray Spectroscopy. *Steel Res. Int.* **2020**, *91*, 1900477. [[CrossRef](#)]
9. Peymandar, M.; Schmuck, S.; Von Schweinichen, P.; Senk, D. Interfacial Reactions between Slag and Melt in the New World of High Manganese Steels. In *EPD Congress 2014*; Wiley: Hoboken, NJ, USA, 2014; pp. 291–298.
10. Deng, Z.; Kong, L.; Liang, N.; Zhu, M. Reaction of Al-Killed Manganese Steel with Ladle Slag. *Steel Res. Int.* **2019**, *90*, 1800480. [[CrossRef](#)]
11. Li, M.; Yu, H.; Pan, M.; Bai, H. Effect of Refining Slag on Non-metallic Inclusions in High Manganese Steel. *Iron Steel* **2019**, *54*, 37–42. [[CrossRef](#)]
12. Yu, H.; Yang, D.; Li, M.; Zhang, N. Effects of Al Addition on the Reaction between High-Manganese Steel and CaO-SiO₂-Al₂O₃-MgO Slag. *Steel Res. Int.* **2020**, *91*, 2000143. [[CrossRef](#)]
13. Yu, H.-X.; Wang, X.-H.; Zhang, J.; Wang, W.-J. Characteristics and metallurgical effects of medium basicity refining slag on low melting temperature inclusions. *J. Iron Steel Res. Int.* **2015**, *22*, 573–581. [[CrossRef](#)]
14. Ji, Y.; Liu, C.; Yu, H.; Deng, X.; Huang, F.; Wang, X. Oxygen Transfer Phenomenon between Slag and Molten Steel for Production of IF Steel. *J. Iron Steel Res. Int.* **2020**, *27*, 402–408. [[CrossRef](#)]
15. Ji, Y.; Liu, C.; Lu, Y.; Yu, H.; Huang, F.; Wang, X. Effects of FeO and CaO/Al₂O₃ Ratio in Slag on the Cleanliness of Al-Killed Steel. *Met. Mater. Trans. A* **2018**, *49*, 3127–3136. [[CrossRef](#)]
16. Suito, H.; Inoue, R. Thermodynamics on Control of Inclusions Composition in Ultra-clean Steels. *ISIJ Int.* **1996**, *36*, 528–536. [[CrossRef](#)]
17. Yu, H.; Xu, J.; Zhang, J.; Wang, X. Effect of Al₂O₃ content on metallurgical characteristics of refining slag. *Ironmak. Steelmak.* **2016**, *43*, 607–615. [[CrossRef](#)]
18. Sigworth, G.K.; Elliott, J.F. The Thermodynamics of Liquid Dilute Iron Alloys. *Met. Sci.* **1974**, *8*, 298–310. [[CrossRef](#)]
19. Park, J.H.; Kim, D.S. Effect of CaO-Al₂O₃-MgO Slags on the Formation of MgO-Al₂O₃ Inclusions in Ferritic Stainless Steel. *Metall. Mater. Trans. B* **2005**, *36*, 495–502. [[CrossRef](#)]
20. Elliott, J.F.; Gleiser, M.; Ramakrishna, V. *Thermochemistry for Steelmaking*; Addison-Wesley: London, UK, 1963.
21. Hino, M.; Ito, K. *Thermodynamic Data for Steelmaking*; Tohoku University Press: Sendai, Japan, 2010.
22. Kim, D.J.; Park, J.H. Interfacial Reaction Between CaO-SiO₂-MgO-Al₂O₃ Flux and Fe-xMn-yAl (x = 10 and 20 mass pct, y = 1, 3, and 6 mass pct) Steel at 1873 K (1600 °C). *Metall. Mater. Trans. B* **2012**, *43*, 875–886. [[CrossRef](#)]
23. Ohta, H.; Suito, H. Activities of MnO in CaO-SiO₂-Al₂O₃-MnO (<10 Pct)-FeO(<3 pct) slags saturated with liquid iron. *Metall. Mater. Trans. B* **1995**, *26*, 295–303. [[CrossRef](#)]
24. Chen, J. *Data Manual for Charts Commonly used in Steelmaking*; Metallurgical Industry Press: Beijing, China, 2010.